FTIR Spectroscopic and Density Functional Model Cluster Studies of Methane Adsorption on MgO

A. M. Ferrari,[†] S. Huber,[‡] H. Knözinger,[‡] K. M. Neyman,[†] and N. Rösch*,[†]

Lehrstuhl für Theoretische Chemie, Technische Universität München, 85747 Garching, Germany, and Institut für Physikalische Chemie, Universität München, Sophienstrasse 11, 80333 München, Germany

Received: November 5, 1997; In Final Form: March 13, 1998

Methane adsorption on the MgO surface has been studied by combining FTIR spectroscopy and density functional (DF) cluster model calculations. Different configurations for the adsorbed methane molecule have been computationally investigated on both Lewis acid and basic surface centers located at the (100) planar surface and at the low-coordinated surface sites (edge and corner). Methane has been found to be very weakly bound on the MgO surface and mainly at the low-coordinated ions. Upon interaction with the surface, the C−H symmetric stretching mode (IR symmetry forbidden for the free molecule) becomes IR active and shifts toward lower frequencies. To account for the role of Lewis acid sites in methane adsorption, CO coadsorption has been also considered.

1. Introduction

Recently, utilization of natural gas, especially the conversion of methane to chemical products such as ethylene and methanol, has been widely studied.[1] In particular, the oxidative coupling of methane has attracted considerable attention.[2−4] Many metal-oxide catalysts have been synthesized for this reaction,[5−9] and Li-doped MgO has been found to be one of the most active.[6,8,10] When methane is passed over MgO at temperatures above 800 K, CH_3 radicals are formed, which are released into the gas phase and detected after collection in an argon matrix.[5,7] Thus, the abstraction of hydrogen from CH_4 by the surface has been experimentally verified. The active sites for the process have been studied extensively and discussed controversially.[4] The rate-determining step in the conversion of methane to higher derivatives has been shown to be hydrogen abstraction by surface sites.[6,11] Irrespective of the detailed mechanism of the coupling reaction, the dissociation of methane is generally accepted as the initial step,[4] and several theoretical works have been devoted to the study of the dissociative chemisorption of methane on O^- centers of Li-doped MgO.[12−16]

The following mechanism of CH_4 chemisorption has been proposed by Ito and co-workers.[17−19] They found that on MgO pretreated above 973 K methane can adsorb in a heterolytically dissociated form, CH_3^- on Mg^{2+} and H^+ on O^{2-}, even below room temperature.[17−19] An active site for this low-temperature adsorption consists of low-coordinated surface ions formed by high-temperature pretreatment in a vacuum. This finding was supported by ab inito calculations carried out for a Mg_4O_4 cluster model.[19,20]

Since it is difficult for methane to be captured by the surfaces of metal oxides, the nature of the interaction of methane with surface sites is still far from being understood. The adsorption of methane on various oxides was investigated by FTIR spectroscopy at 173 K,[21] and the authors found different types of adsorbed molecular species. Methane has been considered to be preferentially bound at the Lewis basic sites on MgO, but also CH_4 adsorbed on a Lewis acid−base pair has been proposed as a possible precursor for methane activation. Unfortunately, these suggestions have not been supported by quantum chemical calculations.

Despite the great interest in and importance of the identification of methane adsorption sites on the MgO surface, to the best of our knowledge, no comprehensive theoretical works have been recently devoted to this problem. Thus, to gain more information about adsorption sites on MgO surfaces and on the configuration of methane molecularly adsorbed at low temperatures, in the present contribution the CH_4 interaction with the MgO surface has been investigated by combining FTIR experiments and density functional (DF) cluster model calculations.

By analyzing experimental and computed results we intend to clarify several open questions about CH_4 adsorption on an MgO surface: (i) which adsorption sites are favorable? (ii) which are the energetically preferred configurations of adsorbed methane molecules? (iii) what is the role of low-coordinated surface sites in methane adsorption? (iv) which are the IR spectroscopic features of adsorbed methane and how can they be rationalized? Moreover, CO coadsorption with CH_4 on MgO has also been considered; the present experimental and computational results are discussed in the light of hypotheses proposed in the literature. A novel rationalization of CO and CH_4 coadsorption on MgO is suggested.

2. Experimental Section

For FTIR spectroscopy, self-supporting wafers of MgO were pressed with a pressure of 15 MPa for 10 min. The resulting wafers (15 mg/cm^2) were pretreated in situ in an oxygen stream at 773 K for 1 h, followed by evacuation ($\sim 10^{-3}$ Pa) at 773 K for 1 h. Prior to admission of methane, the wafer was cooled with liquid nitrogen to 88 K. IR transmission spectra were recorded as a function of equilibrium pressure of the adsorbate using a Bruker IFS66 FTIR spectrometer with a spectral resolution of 0.7 cm^{-1}. Two hundred fifty-six scans were accumulated. A detailed description of the low-temperature

* Corresponding author.
[†] Lehrstuhl für Theoretische Chemie.
[‡] Institut für Physikalische Chemie.

S1089-5647(98)00100-X CCC: $15.00
Published on Web 05/19/1998

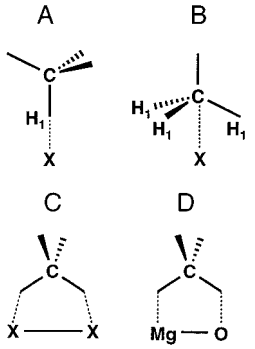

Figure 1. Possible configurations for CH_4 adsorption on an MgO surface; X = Mg or O.

transmission cell has been reported previously.[22] MgO was prepared as described elsewhere,[23] and the specific surface area of this material (35 m^2/g) was determined by nitrogen adsorption.

3. Methods and Models of Calculations

Methane adsorption on the MgO surface has been investigated for different adsorbate coordinations as sketched in Figure 1. Interaction with both Mg^{2+} and O^{2-} surface sites has been analyzed. Since the MgO surface exhibits a large amount of morphological defects (edges, steps, corners, kinks) characterized by a lower coordination of the surface ions,[24] methane adsorption has been studied on different MgO sites: regular planar (100) surface sites formed by five-coordinated ions; edge sites where the surface ions are four-coordinated and corner sites characterized by three-coordinated ions.

Methane interaction has been studied with the help of a cluster approach.[25] This strategy has been widely used to study adsorption and reaction of gas-phase molecules on oxide surfaces and has been found to reproduce in an accurate way electronic structure and binding properties of surface complexes.[24,26−28] Due to the highly ionic nature of MgO, the truncation of the lattice in cluster calculations implies the use of an external field to represent the long-range Coulomb potential. The model clusters considered have been embedded in large arrays of point charges (PC = ±2 au) in order to reproduce the correct Madelung potential at the adsorption site under study.[29] To avoid artificial polarization of ions at the cluster border caused by the lack of the exchange repulsion from neighboring PCs (an effect that is much more pronounced for the more diffuse and easily polarizable oxygen anions), all nearest-neighbor positive PCs around the cluster have been replaced by TIMPs (total ion model potential).[30] TIMPs provide a representation of the core electron density of Mg^{2+} and the exchange repulsion between electrons of O^{2-} at the cluster border and the surrounding.

Two different clusters have been used to represent the (100) planar surface of MgO: (i) the cluster models Mg_5O_5 and O_5-Mg_5 (Figure 2, structure **c**) centered on the Mg^{2+} and on O^{2-} ions in the first layer have been chosen to describe configurations **A** and **B** of methane on Mg^{2+} and O^{2-} centers, respectively (Figure 1); (ii) the cluster $Mg_{12}O_{12}$ (Figure 2, structure **d**) has been employed to model structures of type **C** and **D** (Figure 1). For edge and corner sites, only configurations **A** and **B** have been investigated; the edge sites have been modeled using the clusters Mg_6O_6 and O_6Mg_6 (Figure 2, structure **b**) and the corner sites using the clusters Mg_4O_4 and O_4Mg_4 (Figure 2, structure **a**).

All calculations have been performed at the DF level of theory using the LCGTO-DF (linear combination of Gaussian-type

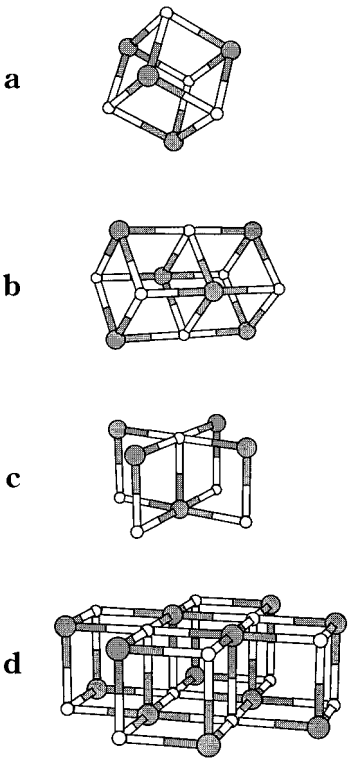

Figure 2. Cluster models used to describe the MgO surface. Large spheres: O, small spheres: Mg. Models for CH_4 configurations **A** and **B** on Mg^{2+} sites (see also Figure 1): (a) Mg_4O_4 for corner sites, (b) Mg_6O_6 for edge sites, (c) Mg_5O_5 for the (100) planar surface. Analogous O^{2-} surface sites have been modeled by clusters where the positions of cations and anions are interchanged. (d) $Mg_{12}O_{12}$ cluster model used to study CH_4 configurations **C** and **D**.

orbitals DF) package and employing the gradient corrected Becke−Perdew (BP) functional (Becke's exchange functional[31] in combination with the Perdew's correlation functional[32]). Orbital basis sets and contraction coefficients, (15s10p1d) → [6s5p1d] for Mg and (13s8p1d) → [6s5p1d] for O in the MgO cluster models, have been taken from a previous study of transition metal atoms adsorbed on a MgO(100) surface.[33] For the C and O of the adsorbates, (9s5p2d) → [5s4p2d], basis sets have been adopted;[34] for H a (6s2p) → [3s2p] basis set has been used.[34] The auxiliary fitting basis set used in the LCGTO-DF code[35,36] to represent the electron charge density was constructed from the orbital exponents in a standard fashion.[36] Geometries have been optimized automatically using analytical energy gradients. During geometry determination, the structure of the MgO cluster model has been kept fixed at the ideal bulk-terminated lattice values (rock salt structure, d(Mg−O) = 2.104 Å[37]), while all other degrees of freedom have been optimized subject to symmetry restrictions imposed. In some cases, mentioned explicitly below, also relaxation of the top-layer adsorption site has been considered. Harmonic vibrational frequencies have been derived from the force constants computed numerically within a finite difference approach. All binding energies have been corrected for the basis set superposition error (BSSE) using the standard counterpoise technique.[38]

Energies of weak bonds may be slightly underestimated by standard DF approximations mainly because small dispersion contributions are not taken into account, even if gradient corrected exchange-correlation functionals are employed.[39−41] On the other hand, it has been well documented recently that gradient corrected DF methods adequately describe structure and energetics of weakly (but not merely dispersively) bound molecular complexes and, in general, those where electrostatics

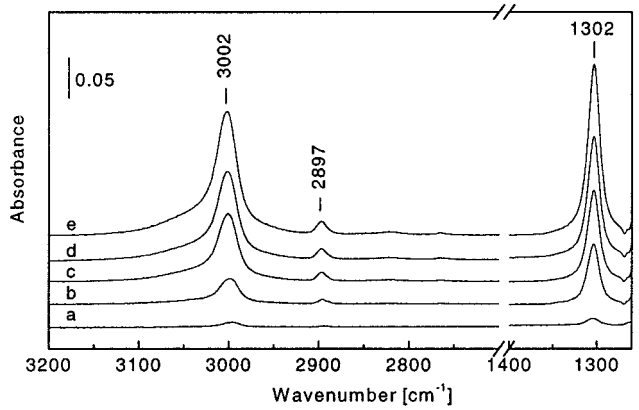

Figure 3. FTIR-spectra of (a) 0.01, (b) 0.02, (c) 0.05, (d) 0.1, and (e) 0.2 kPa CH_4 on MgO at 88 K.

TABLE 1: Vibrational Frequencies of Free CH_4, Observed IR Bands upon CH_4 Adsorption on an MgO Surface and Corresponding Shifts Compared to the Free Molecule (in cm^{-1})

vibrational modes	gas phase[a]	adsorbed on MgO	frequency shift
ν_1 (a_1), symmetric stretch.	2914[b]	2897	−17
ν_2 (e), deformation	1526[b]	not observed	
ν_3 (f_2), antisymmetric stretch.	3020	3002	−18
ν_4 (f_2), deformation	1306	1302	−4

[a] Reference 46. [b] Infrared inactive, Raman band.

dominates.[42,43] DF binding energies of such systems are at least as accurate as MP2 results and often comparable in precision to benchmark data calculated at highly correlated configuration interaction levels.[42−45] Thus, our decision to study methane adsorption on MgO with the help of a DF method is justified for various reasons: the interactions under study are primarily of electrostatic origin (see below), the molecular species involved are rather complex, and, as just discussed, DF methods exhibit a high level of performance for this type of problems.

4. Results

4.1. FTIR Spectroscopic Results. Figure 3 shows FTIR spectra after exposing the pretreated MgO to methane at 88 K. The assignments of the bands of adsorbed methane and a comparison with those of free CH_4 are summarized in Table 1. The isolated molecule is characterized by a triply degenerate C−H antisymmetric stretching mode ν_3 at 3020 cm^{-1} and by a nondegenerate C−H symmetric stretching vibration ν_1 at 2914 cm^{-1}; the two degenerate H−C−H deformation modes ν_2 and ν_4 are at 1526 and 1306 cm^{-1}, respectively.[46] The symmetric stretching mode ν_1 and the deformation mode ν_2 are IR forbidden by symmetry and their frequencies were measured by means of Raman spectroscopy.[46] Upon interaction of methane with the MgO surface, the antisymmetric stretching vibration ν_3 can be seen at 3002 cm^{-1}. The band at 2897 cm^{-1} arises from the symmetric stretching vibration ν_1 which is an infrared forbidden mode in the free CH_4 molecules.[46] The band at 1302 cm^{-1} can be attributed to the ν_4 mode of adsorbed methane. The bands in the hydroxyl region at 3750 and at 3630 cm^{-1} (not shown) are not affected by methane molecules. Adsorbed methane can be easily removed by evacuation. The break-down of the infrared selection rule indicates that the adsorbed methane interacts with the surface so that its T_d symmetry is broken. Symmetry reduction from T_d to C_{3v} can lead to an activation of the infrared forbidden bands ν_1 and ν_2 and to a splitting of the triply degenerate bands ν_3 and ν_4.[46]

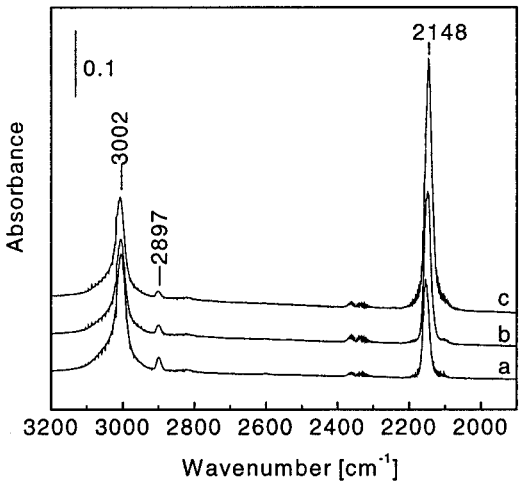

Figure 4. FTIR-spectra of (a) 0.5 kPa CH_4 + 0.5 kPa CO, (b) 0.5 kPa CH_4 + 2 kPa CO, and (c) 0.5 kPa CH_4 + 5 kPa CO on MgO at 88 K.

The activation of the ν_1 mode of adsorbed methane and the frequency shift to lower wavenumbers of all bands provides clear evidence for a reduction of T_d symmetry of methane molecules. Figure 1 shows possible interactions of methane with Lewis acidic and Lewis basic sites of MgO. Due to the fact that at low CH_4 pressure there is no splitting of the modes ν_3 and ν_4 (the half-width of the ν_3 mode is about 30 cm^{-1} at 0.05 kPa CH_4), it is not possible to determine the symmetry of adsorbed methane and therefore to discriminate between different possible adsorption sites.

Li et al.[21] studied the adsorption of methane on differently treated MgO and observed IR bands at 3008, 3000, 2900, 2890, and 1306 cm^{-1}. The high-frequency bands at 3008 and 3000 cm^{-1} were assigned to the degenerate stretching vibration, and those at 2900 and 2890 cm^{-1} were interpreted as originating from the infrared forbidden ν_1 mode. The observed IR bands were attributed to two types of adsorbed methane: one with IR bands at 3008 and 1306 cm^{-1} due to weakly adsorbed methane on surface oxygen anions and another with bands at 3000, 2900, 2890, and 1306 cm^{-1} due to methane interacting with the Lewis acid−base pair sites of MgO. The low surface area of the present MgO (35 m^2/g), the different pretreatment of the sample and therefore the different relative abundance of defect sites, the different temperature at which the experiment was carried out, and the half-width of the observed bands might be reasons for failing to detect a splitting of the antisymmetric mode and several values for the symmetric stretching mode in the spectra. Davydov et al.[47] reported heterolytic adsorption of methane at 573 K, however at liquid nitrogen temperature and at low CH_4 partial pressure dissociation is not expected.

CO has been frequently used as a probe to identify Lewis acid sites of metal oxides and zeolites.[48] CO coordinates in an electrostatic way to cationic sites of the metal oxide which leads to a positive vibrational shift relative to the gas phase (2143 cm^{-1}). To distinguish the surface sites available for the formation of methane species, coadsorption of CH_4 and CO was carried out at 88 K. CO adsorbed on the surface of MgO leads to a band at 2148 cm^{-1} with shoulders at 2155 and 2134 cm^{-1}. The spectra of the coadsorption of 0.5 kPa CH_4 with 0.5, 2, and 5 kPa CO are shown in Figure 4. Adsorption of 0.5 kPa CH_4 gives rise to bands at 3002, 2897, and 1302 cm^{-1}. With increasing CO partial pressure the characteristic C−O stretching vibration at 2148 cm^{-1} is observed which arises from $Mg^{2+}\cdots H_2CO$ interactions. The integral intensities of the C−O stretching bands when CH_4/CO were coadsorbed are comparable

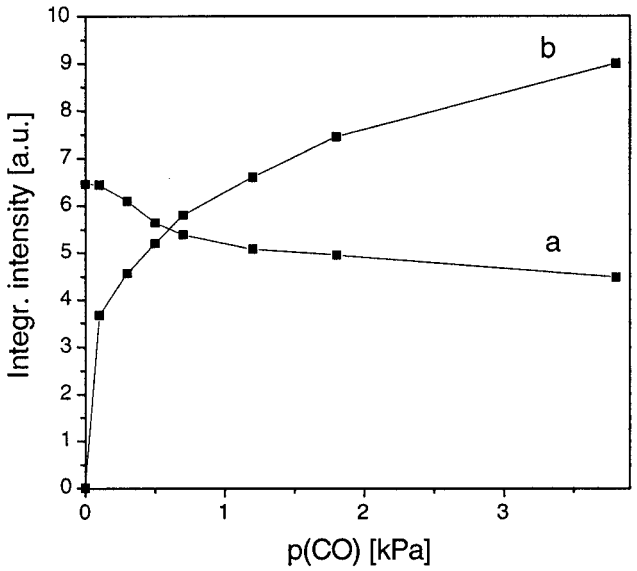

Figure 5. Correlation of the integral intensities of (a) the antisymmetric CH-stretching mode and (b) the CO-stretching mode after CO admission on preadsorbed CH_4 (0.5 kPa) as a function of CO pressure.

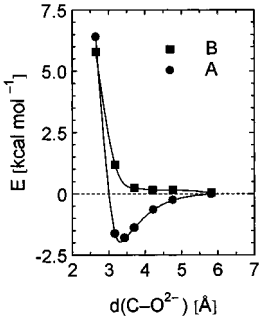

Figure 6. Potential energy curves for CH_4 interaction on the O^{2-} corner site, modeled by the cluster O_4Mg_4, as a function of the distance between the O^{2-} center and the CH_4 carbon atom, $d(C-O^{2-})$. Both CH_4 configurations **A** and **B** have been considered (see Figure 1).

to those of CO adsorbed alone. As shown in Figure 5 the integral intensities of the antisymmetric C−H stretching vibration of adsorbed methane are noticeably reduced (by 37%), while the intensity of the C−O stretching vibration increases with increasing CO pressure. The integral intensities of the deformation vibration ν_4 of adsorbed methane also change by the same magnitude as the antisymmetric stretching vibration ν_3. Different adsorption sites, like the sites on corners, edges, and on the planar surface are available for CH_4 molecules on MgO. As one can see from Figure 5, coadsorption of CO does not lead to a complete disappearance of the vibrational bands of adsorbed methane. Thus, CO can displace CH_4 only from some of the available adsorption centers of MgO surface.

4.2. Results of Cluster Model Calculations. *Methane Interaction with MgO Corner Sites.* The potential energy curves for both **A** and **B** configurations with the O^{2-} site of the O_4Mg_4 model cluster are reported in Figure 6. As shown in the picture, the 3-fold interaction of methane, O_4Mg_4/CH_4 (**B**), with the O^{2-} center is repulsive while the 1-fold configuration, O_4Mg_4/CH_4 (**A**), exhibits a minimum in the potential energy surface at a distance $d(C-O^{2-})$ between the O^{2-} anion and the CH_4 carbon atom of 3.34 Å with a binding energy BE of 1.85 kcal mol^{-1} which decreases to 1.44 kcal mol^{-1} after BSSE correction. This latter structure was completely optimized and results are reported in Table 2. After geometry relaxation of the adsorbed CH_4, the binding energy is reduced by only 0.04 kcal mol^{-1} indicating that very small changes in the geometrical structure of methane have occurred in comparison with the free CH_4 molecule (see Table 2 for geometrical parameters). The intermolecular distance $d(H_1-O^{2-}) = 2.2$ Å is very close to the sum of the O^{2-} ionic radius, $r(O^{2-}) = 1.4$ Å,[49] and the H van der Waals radius, $r_{VdW}(H) = 1.0$ Å,[50] a result also found in the case of other weak interactions.[51]

TABLE 2: Interaction of CH_4 with Mg^{2+} Mg_4O_4 and O^{2-} O_4Mg_4 Corner Sites of the MgO Surface Calculated at the DF(Becke−Perdew) Level[a]

	CH_4 free	Mg_4O_4/CH_4 (B)	Mg_4O_4/CH_4 (A)	O_4Mg_4/CH_4 (A)
d(C−H)	1.099	1.100	1.092	1.102
d(C−H_1)		1.104	1.112	1.106
∠(HCH_1)	107.5	107.0	108.6	110.1
d(C−Mg^{2+})		2.488	3.383	
d(C−O^{2-})				3.339
d(H_1−Mg^{2+})		2.409	2.271	
d(H_1−O^{2-})				2.233
BE		4.13	1.04	1.89
BE_{BSSE}		3.52	0.52	1.48
(ν_4) δ(HCH) (Δ)	1274	1262		1249
		1280		1299
		1267[b] (−7)		1255[b] (−19)
(ν_2) δ(HCH) (Δ)	1498	1500 (+2)		1506 (+8)
(ν_1) $\nu(CH)_s$ (Δ)	2929	2887 (−42)		2869 (−60)
(ν_3) $\nu(CH)_s$ (Δ)	3054	3007		2989
		3049		3015
		3035[b] (−19)		3006[b] (−48)

[a] The MgO clusters are unrelaxed with bulk-terminated geometry; the CH_4 structure is fully optimized under C_{3v} symmetry constraints. Distances d in angstroms, angles in degrees, binding energies BE and BSSE corrected binding energies BE_{BSSE} in kcal mol^{-1}, symmetric $\nu(CH)_s$ and antisymmetric $\nu(CH)_{as}$ C−H stretching modes, and δ(HCH) deformation vibrations, as well as the corresponding shifts Δ (in parentheses) compared to the free molecule in cm^{-1} (see also Figure 1). [b] Average value weighted by the calculated intensities of the splitted modes.

Frequencies of the IR vibrational C−H symmetric, $\nu(CH)_s$, and antisymmetric, $\nu(CH)_{as}$, stretching modes are also shown in Table 2. The most interesting IR spectroscopic features are the activation of the $\nu(CH)_s$ mode (IR forbidden for the free molecule) and the red shifts of both the symmetric and antisymmetric stretching modes; the δ(HCH) deformation mode ν_4 exhibits also a red shift while the δ(HCH) deformation mode ν_2 not observed in the IR spectra, remains almost unaffected by the interaction (Table 2). All computed results are in a qualitative agreement with the experimental findings (Table 1).

For interaction of methane with the cluster Mg_4O_4 representing the Mg^{2+} sites, both Mg_4O_4/CH_4 (**A**) and Mg_4O_4/CH_4 (**B**) complexes have been found to be slightly bound also after BSSE corrections by 0.52 and 3.52 kcal mol^{-1}, respectively. Surprisingly, the corresponding intermolecular distance $d(H_1-Mg^{2+})$ is shorter for complex **A** than for complex **B** for which a considerably stronger attraction has been computed (Table 2). In the latter case, $d(H_1-Mg^{2+}) = 2.4$ Å is longer than the sum of the cationic radius of Mg^{2+}, $r(Mg^{2+}) = 0.72$,[49] and $r_{VdW}(H) = 1.0$ Å, but the corresponding $d(C-Mg^{2+}) = 2.5$ Å is quite close to the sum of Mg^{2+} cationic radius and $r_{VdW}(C) = 1.7$ Å.[50] Thus, for the 3-fold coordination of methane, it is likely the electronic repulsion between the Mg^{2+} surface ion and the methane C atom which prevents a closer approach of the adsorbate. For adduct **A**, $d(H_1-Mg^{2+}) = 2.3$ Å is again much longer than the sum of Mg^{2+} cationic radius and van der Waals radius of H, in agreement with a nearly vanishing interaction calculated for this complex.

It is worth noting that the 3-fold coordination of methane on the Mg^{2+} corner site is more favorable, by about 2 kcal mol^{-1},

compared to the 1-fold coordinated complex. This result is not unexpected as the 3-fold coordination of methane on alkali and alkaline-earth cations in exchanged zeolite systems was found to be the most stable one.[52] The vibrational analysis carried out for the complex Mg_4O_4/CH_4 (**B**) shows activation of the $\nu(CH)_s$ mode and a red shift of both the C−H symmetric and antisymmetric stretching frequencies. Also for this complex the δ(HCH) deformation mode ν_4 exhibits a red shift while the δ(HCH) deformation mode ν_2 is nearly unaffected by the interaction (Table 2). The results are again in a qualitative agreement with the experimental data (Table 1).

For the complexes Mg_4O_4/CH_4 (**B**) and the O_4Mg_4/CH_4 (**A**) the relaxation of the top-layer atom of the adsorption sites also has been considered. On the corner site substantial relaxation occurs and the top-layer ion moves inward (into the substrate) to increase the electrostatic attraction with the neighboring ions,[53] by 0.304 Å (Mg^{2+}) and 0.099 Å (O^{2-}) in agreement with previous calculations.[54,55] As a consequence, the electric field at the adsorption site is reduced and weaker interactions take place. For the complex Mg_4O_4/CH_4 (**B**), the binding energy is slightly diminished from 4.13 to 2.87 kcal mol^{-1} in line with an intermolecular distance $d(C-Mg^{2+}) = 2.556$ Å elongated by 0.069 Å even if, after methane interaction, the Mg^{2+} inward displacement decreased to 0.282 Å. On the other hand, for O_4Mg_4/CH_4 (**A**) where the displacement of the O^{2-} site is almost negligible no noticeable effects on adsorption properties have been computed: BE = 1.77 kcal mol^{-1} and $d(C-O^{2-}) = 3.366$ Å (the O^{2-} inward displacement after interaction is 0.092 Å; cf. Table 2). Therefore, if relaxation of the active site is included adsorption features are changed only insignificantly in agreement with earlier calculations.[55]

Interactions with MgO edge sites. Potential energy curves for interactions of methane with the Mg^{2+} site of the Mg_6O_6 cluster model in both **A** and **B** configurations (Figure 1) are displayed in Figure 7 (top part). The 1-fold coordination is unbound on the cationic site while a local minimum is obtained for 3-fold coordination at a distance $d(C-Mg^{2+})$ of 3.12 Å with a binding energy of 0.89 kcal mol^{-1}. However, the binding energy becomes negative after BSSE correction, $BE_{BSSE} = -0.28$ kcal mol^{-1} (unbound state). Mg^{2+} surface cations of the edge site are known to be displaced inward the cluster by about 0.2 Å.[54,55] Therefore, inclusion of cluster relaxation in the calculations should even increase the repulsive interaction.

The potential energy curves for methane adsorption on the O^{2-} site of the O_6Mg_6 cluster model is sketched in Figure 7 (bottom part). Three-fold coordination on the O^{2-} site is repulsive, while a local minimum has been found for 1-fold configuration at a distance $d(C-O^{2-}) = 3.64$ Å with a binding energy of 0.50 kcal mol^{-1} which almost disappears after BSSE corrections, $BE_{BSSE} = 0.15$ kcal mol^{-1}. The vertical displacement of the top-layer O^{2-} ion is very small, 0.020 Å, and does not affect methane adsorption.

Interactions with MgO (100) Planar Surface. Configurations **A**, **B**, and **C** (Figure 1) have been investigated for methane adsorption on Mg^{2+} site at the MgO (100) planar surface; the resulting potential energy curves are totally repulsive. The potential energy curves for adsorption at the O^{2-} site of the MgO (100) surface have been also computed. For structure **B** the curve is purely repulsive while a local minimum is present in cases **A** and **C**; however, these latter structures become unbound after BSSE corrections ($BE_{BSSE} = -0.41$ and -0.65 kcal mol^{-1}, respectively).

Finally, structure **D** has been investigated. A local minimum has been found at $d(C-Mg^{2+}) = 3.5$ Å with a nearly vanishing binding energy, BE = 0.34 kcal mol^{-1}, which becomes negative after BSSE corrections, $BE_{BSSE} = -0.50$ kcal mol^{-1}. Relaxation of the planar surface has not been considered here as it is known to be negligibly small.[55,56]

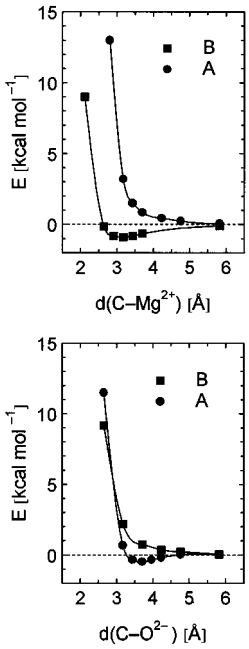

Figure 7. Top part: potential energy curves for CH_4 interaction on the Mg^{2+} edge site, modeled by the cluster Mg_6O_6, as a function of the distance between the Mg^{2+} center and the CH_4 carbon atom, $d(C-Mg^{2+})$. Bottom part: potential energy curves for CH_4 interaction on the O^{2-} edge site, modeled by the cluster O_6Mg_6, as function of the distance between the O^{2-} center and the CH_4 carbon atom, $d(C-O^{2-})$. Both CH_4 configurations **A** and **B** have been considered (see Figure 1).

5. Discussion

According to the calculated results, CH_4 can actually form only a very weak bond with either Mg^{2+} or O^{2-} corner sites. These two complexes, O_4Mg_4/CH_4 (**A**) and Mg_4O_4/CH_4 (**B**), are the most stable ones among those which we have studied (Table 2). On low-coordinated sites where the electrostatic potential is strong, the interaction with Mg^{2+} ions is somewhat more favorable. The analysis of calculated data for these complexes shows an IR activation of symmetric stretching vibrations of CH_4, forbidden in the free molecule, and a red shift of both $\nu(CH)_s$ and $\nu(CH)_{as}$ vibrational bands.

Because correct reproduction of minor energy differences of the order of 1 kcal mol^{-1} is beyond the accuracy limit of the computational method and models adopted here, a very weak attractive interaction of CH_4 on edge and regular planar sites cannot be excluded. In any case, due to the very weak binding on these sites, energy differences between various configurations of adsorbed methane on different adsorption sites are expected to be minute and therefore, a distinction among them is not possible with our present tools; also, it is reasonable to assume hindered rotation of the adsorbate on these sites.

In the case of the complex O_6Mg_6/CH_4 (**A**) on the edge site, for which a very weak binding energy of 0.15 kcal mol^{-1} was calculated, the computed IR frequencies show features similar to those computed for the case of complexes bound at the corner sites: activation of the $\nu(CH)_s$ stretching mode and a red shift in both $\nu(CH)_s$ and $\nu(CH)_{as}$ by -34 and of -28 cm^{-1}, respectively. However, these numbers are to be taken with care and only as an estimate of the shifts induced by the interaction

because, as just mentioned, the value of the computed binding energy is at the limit of the numerical accuracy of the computational method.

On the basis of results discussed until now, it is possible to conclude that computed changes in the IR spectra for various configurations of CH_4 on different sites are dominated by a red shift of both the symmetric and antisymmetric C−H stretching modes. Due to the weakness of the interaction, various adsorption structures exhibit only a small variation in the shift of the stretching modes: in fact the calculated shifts are very close to each other and differ by only 18 and 30 cm^{-1} for the $\nu(CH)_s$ and $\nu(CH)_{as}$ frequencies, respectively. These results are in line with the experimental data to be discussed in the following.

Experimentally the interaction of methane with the surface of MgO leads to an activation of the IR forbidden C−H symmetric stretching mode. The detected band at 2897 cm^{-1} of adsorbed CH_4 on MgO indicates that the interaction with the surface distorts the structure of methane from T_d to a lower symmetry. Because there is no splitting of the antisymmetric C−H stretching mode detectable in the spectra of adsorbed CH_4, a reliable prediction of the symmetry of the adsorbed species is not possible. Furthermore, both the symmetric and the antisymmetric C−H stretching modes are characterized by a quite large half-width of the bands (30 cm^{-1} for $\nu(CH)_{as}$ and 10 cm^{-1} for $\nu(CH)_s$) so that different adsorbed species may be present but not resolved in the spectra.

When CO molecules interact with a methane-preadsorbed MgO surface, the characteristic mode appears in the IR spectra due to the stretching of adsorbed CO; concomitantly, all bands of adsorbed methane are attenuated (Figure 4). As also shown in Figure 5, coadsorbed CO cannot completely substitute preadsorbed methane even after a prolonged exposure in agreement with previous observations.[21] This result indicates that at least two kinds of adsorbed methane species are present at the MgO surface: one that can be replaced by adsorbed CO and another one remaining intact after CO coadsorption. These two methane species have been discussed in the literature[21] as being due to molecules interacting mainly with O^{2-} surface sites (Figure 1, structure **A**), and the other one due to adsorbates more strongly bound at Lewis acid−base pairs composed by adjacent Mg^{2+} and O^{2-} surface ions (Figure 1, structure **D**). It has also been proposed[21] that CO selectively adsorbs on the Mg^{2+} sites removing the methane preadsorbed on Lewis acid sites, while it does not affect methane molecules occupying the O^{2-} Lewis basic sites. In the latter case surface complexes as sketched in Figure 8, structure **A** should be formed.

On the basis of the present computational results the latter interpretation deserves some comments. CH_4 has been found to be bound on both O^{2-} and Mg^{2+} corner sites while no indications for a significant interaction involving a Lewis acid−base pair site are obtained from computed results. (However, as has been already mentioned, a very weak interaction on the edge site and on the planar surface cannot be excluded.) CO molecules interact more strongly with the Mg^{2+} sites of MgO surface than does methane. For example, on the corner site, CH_4 is bound by 3.5 kcal mol^{-1} while CO is bound by about 11 kcal mol^{-1}.[30] CO can interact with Lewis acid sites on corners, edges, and on the planar surface,[57,58] and when admitted onto the surface, it should remove all methane molecules coordinated on Lewis acid centers and, if present, from Lewis acid−base pair sites. CO coadsorption also affects methane adsorption on neighboring O^{2-} MgO surface sites. Let us consider CO interacting with a Lewis acid site and methane

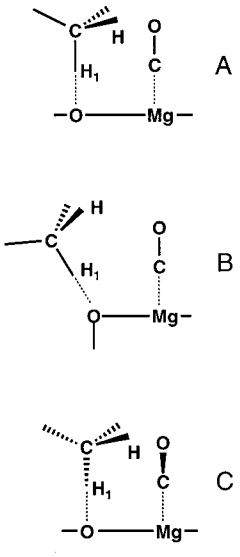

Figure 8. Conceivable configurations for CH_4 and CO coadsorption. **A**, **B**, and **C** display planar, corner, and edge sites, respectively.

TABLE 3: Intermolecular Distances for CH_4 and CO Coadsorption for the Configuration Sketched in Figure 8, structures A−C[a]

distances	structure **A**	structure **B**	structure **C**	sum of VdW radii[b]
$C(CH_4)$−C(CO)	2.3	4.4	3.9	3.4
$C(CH_4)$−O(CO)	2.1	4.7	4.2	3.1
$H_1(CH_4)$−C(CO)	2.3	3.8	3.3	2.7
$H(CH_4)$−O(CO)	1.8	4.2	3.6	2.4
$H_1(CH_4)$−O(CO)	2.1	4.3	3.9	2.4

[a] The sums of the corresponding Van der Waals radii are also reported. All distances in angstroms. [b] VdW radii: $r(H) = 1.0$ Å; $r(C) = 1.7$ Å; $r(O) = 1.4$ Å[50].

with an adjacent Lewis basic site on the planar surface (Figure 8, structure **A**). Assuming reasonable distances between the **C** atom of CH_4 and the O^{2-} anion (3.5 Å) as well as between the **C** atom of CO and the Mg^{2+} cation (2.5 Å), one computes an intramolecular repulsion between the coadsorbed molecules oriented normal to the surface of about 45 kcal mol^{-1}; this strong repulsion is due to distances between coadsorbates which are shorter than the corresponding sum of atomic van der Waals radii (Table 3). This implies that under thermodynamic equilibrium, even if methane is bound on the planar surface, it will be displaced by coadsorbed CO also from the O^{2-} sites.

Repulsion between molecules adsorbed on adjacent sites of morphological defects, where an additional conformational freedom is possible compared to the planar surface, can be significantly reduced and can even become negligible. This is the case, for instance, for methane interacting with Lewis basic corner sites and CO with the nearest Lewis acid edge sites for a presumable configuration as sketched in Figure 8, structure **B**. At the same adsorbate−substrate distance as on the planar surface, the computed intermolecular repulsion can be neglected; it is less than 0.08 kcal mol^{-1} in line with distances between coadsorbates which are longer than the corresponding sum of van der Waals radii (Table 3). Also in the case of CH_4 and CO adsorbed on adjacent O^{2-} and Mg^{2-} edge sites, respectively, it is conceivable that the two molecules tilt out of the symmetry plane of the edge site cluster model, toward opposite sides (Figure 8, structure **C**). For a tilting angle of about 30° each the calculated intermolecular repulsion almost vanishes (about 0.2−0.3 kcal mol^{-1}). Also in this case, the distances between

coadsorbates are considerably longer than the corresponding sum of van der Waals radii (Table 3). Thus on the low-coordinated sites, coadsorbed CO displaces only methane bound at Lewis acid centers, whereas it is possible that methane adsorbed on Lewis basic sites is not removed (Figure 8, structure **B**, **C**).

After CO coadsorption, in fact, the IR intensities of CH_4 bands are reduced by 37% (Figure 5). Since the estimated number of morphological defects may amount up to 30% of all available MgO surface sites,[24] even if methane is also adsorbed on the (100) planar surface, a more pronounced depletion of the corresponding IR signals should be expected as these sites constitute the majority of the available adsorption centers. On the basis of these observations, the hypothesis that CH_4 interacts only with low-coordinated MgO surface sites can be put forward.

6. Conclusions

According to the calculated results, CH_4 is weakly bound on Mg^{2+} and O^{2-} corner sites with adsorption energies of 1−3 kcal mol^{-1}; the interaction is calculated to occur preferentially with Lewis acid sites Mg^{2+}. At cationic sites CH_4 interacts in a 3-fold way, whereas 1-fold coordination is favored at anionic sites. The present computational results support the assumption that methane undergoes hindered rotation at edge sites. At variance with previous assumptions[21] methane has not been found to be bound on the regular, planar MgO (100) surface.

The present spectroscopic and computed data for all adsorption complexes show an activation of the IR symmetric stretching mode of methane induced by adsorption and a red shift of both the symmetric and antisymmetric C−H stretching frequencies. The measured half-width of the C−H stretching bands is large enough (10−30 cm^{-1}) to account for the presence of different complexes of adsorbed methane which display a calculated splitting of at most 30 cm^{-1}.

Adsorption on the (100) MgO planar surface can also be excluded on the basis of the present experimental results for CH_4 and CO coadsorption. Reduction of the integral IR intensity of the antisymmetric C−H stretching vibration shows that only about a third of the preadsorbed methane molecules are displaced by CO. Since CO is more strongly bound on the Lewis acid sites than methane, it displaces methane from these Mg^{2+} sites under thermodynamic equilibrium conditions. At variance with previously proposed models,[21] CO coadsorption also has to affect methane molecules interacting with Lewis basic sites O^{2-} due to the strong repulsion calculated between the coadsorbates when located at adjacent O^{2-} and Mg^{2+} centers on the planar surface. We demonstrated that only if methane is adsorbed on Lewis basic defect sites (low-coordinated O^{2-}) this repulsion can be significantly reduced. Thus, only methane molecules on these lower coordinated sites (corner and edge, Figure 8, structures **B** and **C**), should remain unaffected by CO coadsorption. On the other hand, if CH_4 were bound to regular (100) MgO terraces a much more pronounced reduction of the IR integral intensity of the antisymmetric C−H stretching mode due to CO coadsorption would have been observed, since the (100) planar surface accounts for the majority of available adsorption sites. The picture emerging from both experimental and calculated results is consistent: it shows that CH_4 is adsorbed only at low-coordinated sites.

It appears that methane molecules cannot discriminate between Lewis basic and Lewis acidic sites of MgO at variance with adsorbed CO which is a well-established probe of acidic centers. However, due to the exclusive adsorption affinity of methane for low-coordinated sites, these molecules can perhaps be used to probe the relative amount of morphological defects of MgO samples obtained under different experimental conditions.

Acknowledgment. This work was financially supported by Deutsche Forschungsgemeinschaft, Bayerischer Forschungsverbund Katalyse, and Fonds der Chemischen Industrie.

References and Notes

(1) Keller, G. E.; Bhasin, M. M. *J. Catal.* **1982**, *73*, 9.
(2) Li, C.; Xin, Q. *J. Phys. Chem.* **1992**, *96*, 7714.
(3) Kaliaguine, L.; Shelimov, B. N.; Kazansky, V. B. *J. Catal.* **1978**, *55*, 384.
(4) Lunsford, J. H. In *Handbook of Heterogeneous Catalysis*; Ertl, G., Knözinger, H., Weitkamp, J., Eds.; Wiley-VCH Verlag: Weinheim, 1997; Vol. 4, p 1843.
(5) Driscoll, D. J.; Lunsford, J. H. *J. Phys. Chem.* **1985**, *89*, 4415. Ito, T.; Wang, J.; Lin, C. H.; Lunsford, J. H. *J. Am. Chem. Soc.* **1985**, *107*, 5062.
(6) Hutchings, G. J.; Woodhouse, J. R.; Scurrell, M. S. *J. Chem. Soc., Faraday Trans 1* **1989**, *85*, 2507.
(7) Driscoll, D. J.; Martir, W.; Wang, J.; Lunsford, J. H. *J. Am. Chem. Soc.* **1985**, *107*, 58.
(8) Ito, T.; Lunsford, J. H. *Nature* **1985**, *314*, 721.
(9) Ito, T.; Wang, J.; Lin, C. H.; Lunsford, J. H. *J. Am. Chem. Soc.* **1985**, *107*, 5062.
(10) Lin, C. H.; Ito, T.; Wang, J.; Lunsford, J. H. *J. Am. Chem. Soc.* **1987**, *109*, 4808.
(11) Cant, N. W.; Lukey, C. A.; Nelson, P. F.; Tyler, R. J. *J. Chem. Soc., Chem. Commun.* **1988**, 766.
(12) Orlando, R.; Millini, R.; Perego, G.; Dovesi, R. *J. Mol. Catal.* **1997**, *119*, 253.
(13) Johnson, M. A.; Stefanovich, E. V.; Truong, T. N. *J. Phys. Chem.* **1997**, *101*, 3196.
(14) Børve, K. J.; Pettersson, L. G. M. *J. Phys. Chem.* **1991**, *95*. 7401.
(15) Anchell, J. L.; Morokuma, K.; Hess, A. *J. Chem. Phys.* ***1993***, *99*, 6004.
(16) Yu, J.; Anderson, A. B. *J. Am. Chem. Soc.* **1990**, *112*, 7218.
(17) Ito, T.; Wang, J.; Tashiro, T.; Watanabe, T.; Toi, K.; Ikemoto, I. *Chem. Lett.* **1987**, 1723.
(18) Kobayashi, H.; Yamaguchi, M.; Ito, T. In *Acid-Base Catalysis*; Tanabe, K., Hattori, H., Yamaguchi, T., Tanaka, T., Eds.; Kodansha, Tokyo, 1989.
(19) Ito, T.; Tashiro, T.; Kawasaki, M.; Watanabe, T.; Toi, K.; Kobayashi, H. *J. Phys. Chem.* **1991**, *95*, 4476.
(20) Kobayashi, H.; Yamaguchi, M.; Ito, T. In *Acid-Base Catalysis*; Tanabe, K., Hattori, H., Yamaguchi, T., Tanaka, T., Eds.; Kodansha, Tokyo, 1989.
(21) Li, C.; Li, G.; Xin, Q. *J. Phys. Chem.* **1994**, *98*, 1933.
(22) Kunzmann, G. Dissertation, Ludwigs-Maximilian-Univeristät München, Germany, 1987.
(23) Kirlin, P. S.; Knözinger, H.; Gates, B. C. *J. Phys. Chem.* **1990**, *94*, 8451.
(24) Colbourn, E. A. *Surf. Sci. Rep.* **1992**, *15*, 281.
(25) Pacchioni, G., Bagus, P. S., Parmigiani, F., Eds. *Cluster Model for Surface and Bulk Phenomena*; NATO ASI Series B; Plenum Press: New York 1992; Vol. 283.
(26) Sauer, J.; Ugliengo, P.; Garrone, E.; Saunders, V. R. *Chem. Rev.* **1994**, *94*, 2095.
(27) Lambert, R. M., Pacchioni, G., Eds. *Chemisorption and Reactivity on Supported Clusters and Thin Films*; NATO ASI Series E 331; Kluwer: Dordrecht, 1997.
(28) Neyman, K. M.; Pacchioni, G.; Rösch, N. In *Recent Development and Applications of Modern Density Functional Theory*; Theoretical and Computational Chemistry; Seminario, J., Ed.; Elsevier: Amsterdam, 1996; Vol. 4., p 569.
(29) Pacchioni, G.; Ferrari, A. M.; Marquez, A. M.; Illas, F. *J. Comput. Chem.* **1997**, *18*, 617.
(30) Yudanov, I. V.; Naslusov, V. A.; Neyman, K. M.; Rösch, N. *Int. J. Quantum Chem.* **1997**, *165*, 975.
(31) Becke, A. D. *Phys. Rev. A* **1988**, *38*, 3098.
(32) Perdew, J. P. *Phys. Rev. B* **1986**, *33*, 8622; erratum ibid. **1986**, *34*, 7406.
(33) Yudanov, I.; Pacchioni, G.; Neyman, K.; Rösch, N. *J. Phys. Chem. B* **1997**, *101*, 2786.
(34) Neyman, K. M.; Strodel, P.; Ruzankin, S. P.; Schlensog, N.; Knözinger, H.; Rösch, N. *Catal. Lett.* **1995**, *31*, 273.
(35) Rösch, N. In *Cluster Model for Surface and Bulk Phenomena*, Pacchioni, G., Bagus, P. S., Parmigiani, F., Eds.; NATO ASI Series B; Plenum Press: New York, 1992; Vol. 283, p 251.

(36) Dunlap, B. I.; Rösch, N. *Adv. Quantum Chem*. **1990**, *21*, 317.
(37) Wyckoff, R. W. G. *Crystal Structures*, 2nd ed.; Interscience Publishers: New York, 1965; Vol 1.
(38) Boys, S. F.; Bernardi, F. *Mol. Phys.* **1970**, *19*, 553.
(39) Pérez-Jordá, J. M.; Becke, A. D. *Chem. Phys. Lett*. **1995**, *233*, 134.
(40) Lundqvist, B. J.; Andersson, Y.; Shao, H.; Chan, S.; Langreth, D. C. *Int. J. Quantum Chem.* **1995**, *56*, 247.
(41) Kristyán, S.; Pulay, P. *Chem. Phys. Lett.* **1994**, *229*, 175.
(42) Civalleri, B.; Garrone, E.; Ugliengo, P. *J. Mol. Struct. (THEOCHEM)* **1997**, *419*, 227 and references therein.
(43) Ferrari, A. M.; Ugliengo, P.; Garrone, E. *J. Chem. Phys.* **1996**, *105*, 4129.
(44) Novoa, J. J.; Sosa, C. *J. Phys. Chem.* **1995**, *99*, 15837.
(45) Sim, F.; St-Amant, A.; Papai, I.; Salahub, D. R. *J. Am. Chem. Soc*. **1992**, *114*, 4391.
(46) Herzberg, G. *Molecular Spectra and Molecular Structure*; Van Nostrand Reinhold: New York, 1945; Vol. II (Infrared and Raman Spectra of Polyatomic Molecules).
(47) Davydov, A. A.; Budneva, A. A.; Aliev, S. M.; Sokolovskii, V. D. *React. Kinet. Catal. Lett.* **1988**, *36*, 491.
(48) Knözinger, H. In *Handbook of Heterogeneous Catalysis*; Ertl, G., Knözinger, H., Weitkamp, J., Eds.; Wiley-VCH Verlag: Weinheim, 1997; Vol. 2, p 707.
(49) Shannon, R. D. *Acta Crystallogr*. **1976**, *A32*, 751.
(50) *Periodensystem der Elemente*; VCH Verlag: Weinheim, 1995.
(51) Ferrari, A. M.; Ugliengo, P.; Garrone, E. *J. Chem. Phys.* **1996**, *105*, 4129.
(52) Ferrari, A. M.; Neyman, K. M.; Huber, S.; Knözinger, H.; Rösch, N. Submitted for publication.
(53) Sousa, C.; Mejías, J. A.; Pacchioni, G.; Illas, F. *Chem. Phys. Lett*. **1996**, *249*, 123.
(54) Pacchioni, G.; Minerva, T.; Bagus, P. S. *Surf. Sci.* **1992**, *275*, 344.
(55) Neyman, K. M.; Rösch, N. *Surf. Sci.* **1993**, *297*, 223.
(56) Pope, S. A.; Guest, M. F.; Hillier, I. A.; Colbourn, E. A.; Mackrodt, W. C.; Kendrick, J. *Phys. Rev. B* **1983**, *23*, 1869.
(57) Nygren, M. A.; Petterson, L. G. M. *J. Chem Phys*. **1994**, *110*, 2010.
(58) Escalona-Platero, E.; Scarano, D.; Spoto, G.; Zecchina, A. *Faraday Discuss. Chem. Soc*. **1985**, *80*, 183.